Elastic scattering of electrons by water molecules at intermediate and high energies

Arvind Kumar Jain and A. N. Tripathi
Department of Physics, University of Roorkee, Roorkee 247 667, India

Ashok Jain
Physics Department, Cardwell Hall, Kansas State University, Manhattan, Kansas 66506

(Received 6 July 1987)

Elastic differential, integral, and momentum-transfer cross sections are reported for the scattering of electrons by water molecules in the energy range of 100–1000 eV. A parameter-free model optical potential which is the sum of three spherical terms, namely the static, exchange, and polarization forces, is constructed from near–Hartree-Fock one-center-expansion water wave functions. The total optical potential is then treated exactly in a partial-wave analysis using the variable-phase approach to yield the scattering phase shifts. We employ several versions of parameter-free polarization and exchange potentials. We find that the present calculated differential cross sections reproduce all the important features (such as forward peaking, dip at middle angles, and enhanced backward scattering) observed in recent experiments. Quantitatively, the present results are in very good agreement with experiment and better than earlier calculations.

INTRODUCTION

This work is inspired by the recent measurements[1,2] on the elastic differential cross sections (DCS's) over a wide range of energies for electron-H_2O collisions. Nishimura (cited in Ref. 2) has reported the same scattering parameters at electron energies of 30 and 90 eV. A number of comprehensive review articles dealing with various theoretical[3] approaches and experimental[4] techniques have been published in recent years. Earlier experimental studies on the e-H_2O system have been summarized in Refs. 4 and 5. Interaction of electrons with water molecules (H_2O) plays an important role in the fields of radiation chemistry and space science.[6] Very recently, Shyn and Cho[7] have reported measurements on the absolute DCS's for the e-H_2O system at 2.2–20 eV from 15° to 150°.

On the theoretical side, the DCS have been calculated for this system in the first-Born[8,9] and Glauber[10] approximations at intermediate and high energies. As expected, the results of the first-Born and the Glauber approximations agree with the experimental values only near forward angles and differed significantly in the backward direction both in magnitude and shape. Recently, Katase *et al.*[1] have calculated the elastic DCS, integral (σ_i), and momentum-transfer (σ_m) cross sections using the partial-wave method employing a double Yukawa potential as well as a spherically symmetric static potential for the e-H_2O system derived from the molecular charge density obtained from the molecular-orbital (MO) theory. Their calculated elastic DCS, using a model potential, reproduced the experimental values fairly well except in the forward direction (this is expected since they neglected polarization). In recent years, the spherical-complex-optical-potential (SCOP) model (see Jain[11,12] and Jain *et al.*[13]) has been used to calculate the total (elastic + absorption), momentum-transfer, and differential cross sections for electrons colliding with CH_4 and SiH_4 molecules from very low [near the Ramsaur-Townsend (RT) minimum] to intermediate (near shape-resonance phenomena) and high energies. The success of the SCOP model lies in the fact that the nonspherical interaction terms (such as the dipole, quadrupole, etc.) are either zero or their effect is very small. The success of the SCOP model for e-CH_4 and e-SiH_4 has prompted us to examine the validity of this approach to study the elastic scattering for nonspherical targets at higher energies ($E \geq 100$ eV) where the contribution of dipole, quadrupole, etc. terms is small. In the present study the total interaction between the electron-molecule system is approximated by an optical potential composed of three local and real terms, namely, the static (V_{st}), the exchange (V_{ex}), and the polarization (V_p), involving no adjustable parameter. All three potentials, i.e., the static, exchange, and polarization have been computed from the charge density of the target computed *ab initio* at each radial distance from the center of mass of the H_2O molecule. Thus, the present work differs in two ways from the calculations of Katase *et al.*: first, the static potential is evaluated differently, and second, we include polarization and exchange effects without involving any adjustable parameter.

THEORETICAL METHODOLOGY

The water molecule belongs to the C_{2v} symmetry point group (electronic $^1A_1$ ground state) with the electronic configuration, $1a_1^2 2a_1^2 3a_1^2 1b_1^2 1b_2^2$. A single-center expansion technique (see Thompson and Gianturco[14]) with an oxygen atom at the center is employed for all orbitals in the near-Hartree-Fock limit using experimental values for the nuclear geometry (bond length = 1.792 a.u. and bond angle = 104.5°). The central quantity in the calcula-

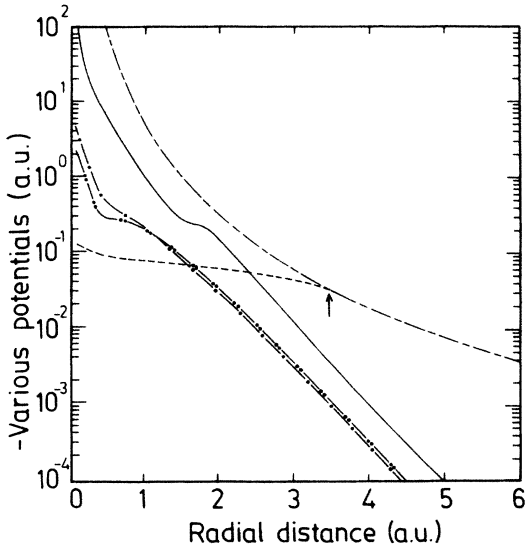

FIG. 1. Various components of the e^--H_2O interaction potential. ——, static potential; — — —, correlation-polarization potential; —·—·—, asymptotic polarization potential; —·—, HFEGE (at 100 eV); —··—, MSCE (at 100 eV).

tions of the optical potential is the charge density $\rho(\mathbf{r})$. The charge density $\rho(\mathbf{r})$ was calculated (for details, see Ref. 14) from the single-center wave function with enough terms in the expansion of each bound orbital. The $\rho(\mathbf{r})$ is then expanded in terms of symmetry-adapted functions belonging to the symmetric A_1 irreducible representation of the molecular C_{2v} point group, i.e.,

$$\rho(\mathbf{r})=\Sigma\bar{\rho}_{LH}(r)X_{LH}^{A_1}(\hat{\mathbf{r}}) . \tag{1}$$

In the spherical approximation,[11,12] we need only the first term ($L=0, H=1$) of the expansion Eq. (1) in order to evaluate all the three local potentials, i.e., V_{st}, V_{ex}, and V_p. Explicit expressions for $V_{st}(r)$ and $V_{ex}(r)$ [Hara-free-electron-gas-exchange (HFEGE) potentials] are given in the literature (see, for example, Gianturco and Jain[3]). The modified-semiclassical-exchange (MSCE) potential for $V_{ex}(r)$ is taken from Gianturco and Scialla.[15] The correlation-polarization potential (COP) for the e-H_2O system is calculated following Padial and Norcross[16] and Gianturco *et al.*[17] At larger distances the COP $V_p(r)$ is replaced by the correct asymptotic form $-\alpha_0/2r^4$ (α_0 is the dipole polarizability of H_2O; we use the experimental value of 9.83 a.u. for α_0) where they cross each other for the first time (the crossing point occurs at 3.4 a.u., see arrow in Fig. 1). It is well known that as the energy increases nonadiabatic effects become important and so they should be taken into account. Consequently we have also considered an energy-dependent Buckingham-type polarization potential[18,19]

$$V_p(r)=-\frac{\alpha_0 r^{2n-4}}{2(r^2+r_c^2)^n}, \quad n=2,3,4 \tag{2}$$

where r_c is the cutoff parameter determined from the relationship[20]

$$r_c=\frac{3}{8}\frac{k}{\Delta} ,$$

where Δ is the mean excitation energy obtained in the closure approximation[20] from the ground-state target wave function ψ_0,

$$\Delta=\frac{2\langle\psi_0|Z^2|\psi_0\rangle}{\alpha_0} .$$

For H_2O, Δ is calculated to be 18.68 eV.

It is now a standard procedure to compute the lth partial-wave phase shift from the solutions of the following second-order differential equation:

$$\left[(d^2/dr^2)+k^2-\frac{l(l+1)}{r^2}-V_{ex}(r)-V_{st}(r)-V_p(r)\right]f_l(kr)=0 , \tag{3}$$

where k^2 is the electron energy. We employ a variable-phase approach (VPA) (Ref. 21) to find the solution of Eq. (3). The corresponding quantities (σ_t, σ_m, and DCS) are then easily obtained from the S matrix at each energy. All our cross sections are converged with respect to the number of partial waves up to a value of 0.001 rad only.

RESULTS AND DISCUSSION

Before we present our calculations on the cross sections it is worthwhile to examine the behavior of the radial shapes of the various potentials. They are displayed in Fig. 1. The static interaction dominates all other interactions (exchange and polarization) up to $r=2.4$ a.u. well outside the region of the H nuclei. Beyond this distance the correlation polarization takes over both the static and exchange interactions. The exchange term remains weaker than the static interaction up to a very large r value ($r\simeq 8.25$ a.u.). It is also seen that at these energies, i.e., $E\geq 100$ eV, the V_{ex} (MSCE) and V_{ex}(HFEGE) potentials are quite similar to each other except at small values of r (see Fig. 1).

In Fig. 2 we compare the present $\rho(r)$ with the values of Katase *et al.* using both their double Yukawa (DY)

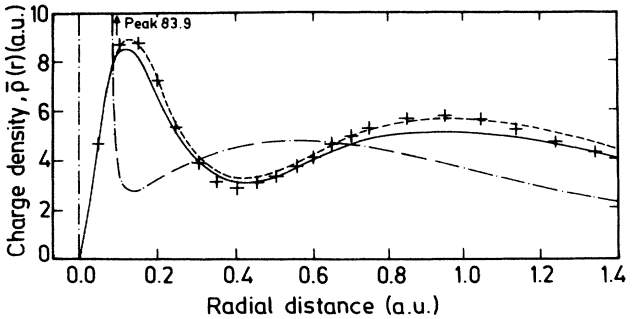

FIG. 2. Spherical charge density $\overline{\rho(r)}$ of the H_2O molecule. ——, values used in this work (Ref. 14); — — —, calculations of Banyard and March using the MO wave function (Ref. 25); +, analytic fitting with parameters (Ref. 1); —·—, using a double-Yukawa-type potential (Ref. 1).

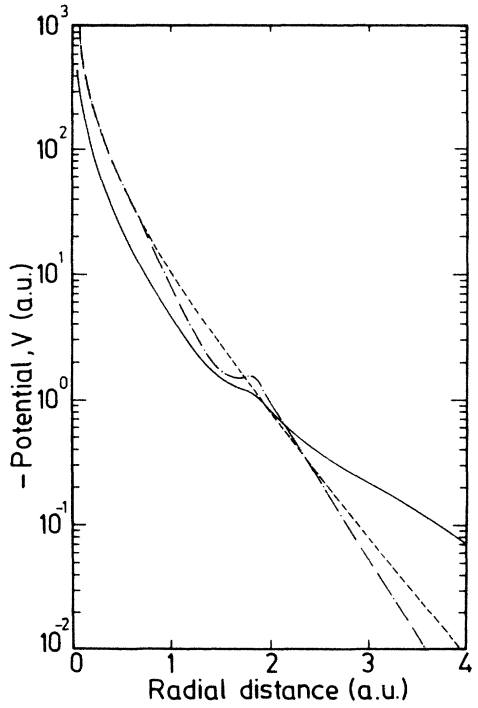

FIG. 3. Spherically symmetric potentials for e^--H_2O scattering used to calculate the final cross sections. ——, present sum of $V_{st}+V_{ex}+V_p$ at 100 eV; — — —, with realistic potential by Katase *et al.* (Ref. 1); –·– with double Yukawa potential (Ref. 1).

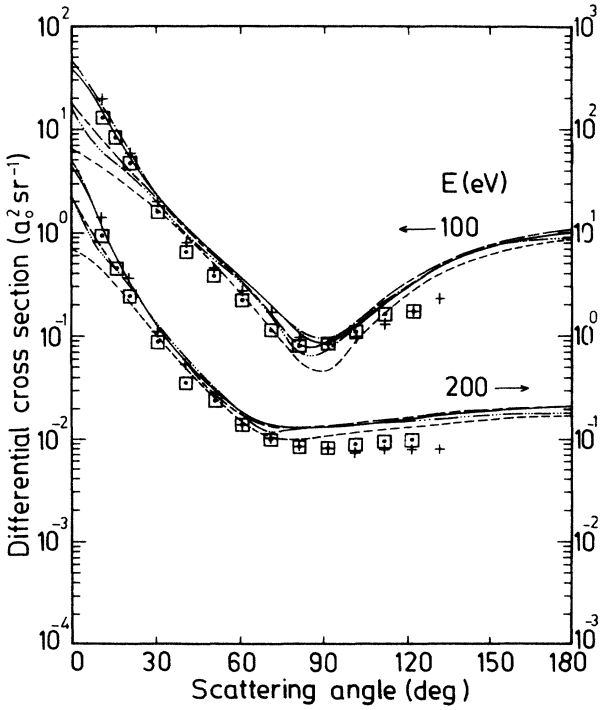

FIG. 4. Differential cross sections for e^--H_2O scattering at 100 and 200 eV. Present calculations: ——, *SHP*1 model; –·–, *SEP*1 model; ——, *SHP*2 model; –···–, *S* model (for notations see the text); — — —, theoretical results of Katase *et al.* (Ref. 1). Experimental data: +, Katase *et al.* (Ref. 1); □, Danjo and Nishimura (Ref. 2) (note the arrows for scale).

potential and MO theory. It is clearly seen that the $\rho(r)$ reported by Katase *et al.* using MO theory has two maxima at values of $r=0.1$ and 1.0 a.u. and is in complete agreement with the present calculations. On the other hand, the $\rho(r)$ obtained with the DY potential is very different giving the peaks at $r=0.014$ and 0.5 a.u. From the knowledge of the charge density $\rho(r)$, we can easily reproduce the nature of the potential function (for example, see Fig. 3). It is surprising to see that the DY potential is not very different from their so-called realistic potential (Ref. 1) estimated from the charge distribution obtained from MO theory in the entire region of r, although their respective charge densities differ considerably. This indicates that one should be careful in using the empirical potential in the model calculations and therefore, we compare our results with the results of Katase *et al.* obtained by using their realistic potential only. Our parameter-free *ab initio* interaction which includes static, exchange, and correlation-polarization forces matches well in shape but not in magnitude the realistic potential curve of Katase *et al.* (Fig. 3). The large magnitude of our total interaction $V(r)$ is due to the inclusion of other components of interaction like $V_{ex}(r)$ and $V_p(r)$. This is borne out by the fact that the present $V_{st}(r)$ interaction compares well both in shape and magnitude with their realistic potential. We now discuss our results on the scattering parameters.

A. Differential cross sections (DCS's)

Figures 4–6 display our DCS's in the energy range 100–1000 eV. Note that in the present model the DCS's at the zero angle are undefined; therefore, the zero-angle points in Figs. 4–6 should not be taken seriously. We have calculated the DCS in various models abbreviated as follows: *S*, static potential; *SH*, *S* plus the HFEGE potential; *SHP*1, *SH* plus the correlation polarization potential; *SHP*2, *SH* plus the energy-dependent polarization potential [Eq. (2)]; *SE*, *S* plus the MSCE potential; *SEP*1, *SE* plus the correlation-polarization potentials. We have also shown on each curve the experimental data as well as the model calculations of Katase *et al.*[1] The measured values of Danjo and Nishimura are shown only at 100 and 200 eV whereas Lassettre's and White's[22] and Bromberg's (cited in Lassettre and White) measurements are shown only in the forward direction at 500 eV.

Figure 4 shows our DCS results at 100 and 200 eV. At 100 eV, as expected, the *SHP*1 and *SEP*1 curves yield similar DCS's in the entire angular region, both giving the forward peak and a broad minima around 80°–100°. The present model calculations (*SHP*1 and *SEP*1) are in good agreement with the measured values of Katase *et al.*[1] and Danjo and Nishimura[2] both at small angles ($\theta \lesssim 30°$) and at intermediate angles (80°–100°), i.e., around the dip structure. Beyond 100°, the present calculated DCS values show a large backward peaking slope compared to the measurements which are only available up to scattering angle 120°. At this energy, the Katase *et al.*[1] data are larger by 8–40 % than those of Danjo and Nishimura[2] over all angles.

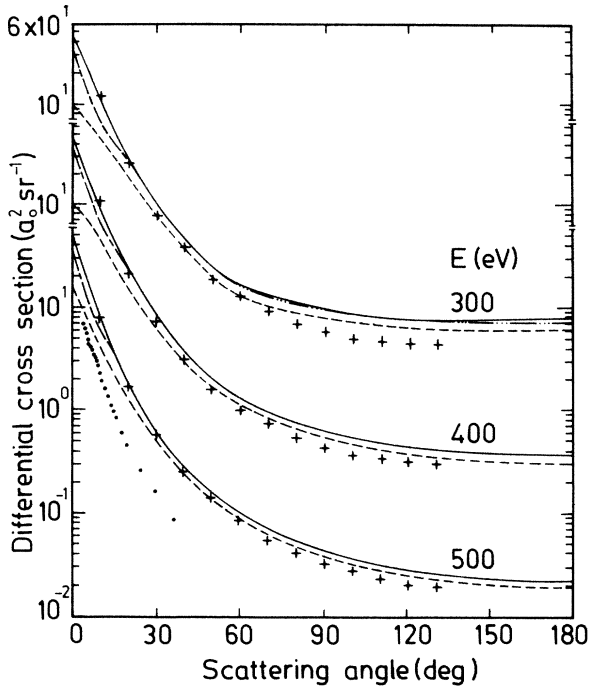

FIG. 5. Same legend as in Fig. 4, but for energies of 300, 400, and 500 eV. Experimental data of Lassettre and White (Ref. 22) are shown by the dotted line.

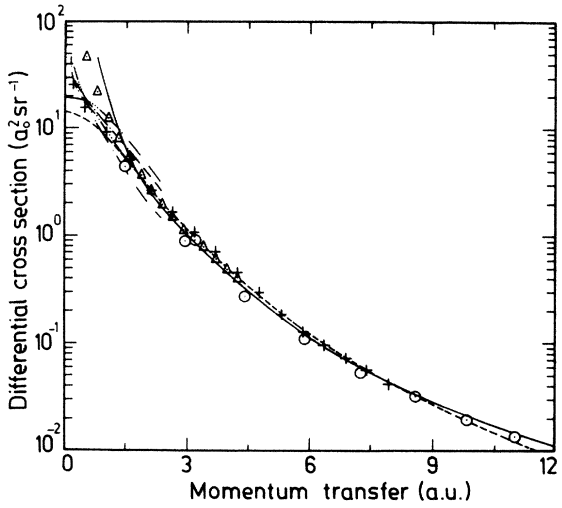

FIG. 7. Differential cross sections for e^--H_2O collisions as a function of momentum transfer. ——, present *SHP*1 calculations at 1000 eV. Results in Born approximation: — — —, Katase *et al.* (Ref. 1); –·–, Sharma and Tripathi (Ref. 26); –··–, Szabo and Ostlund (Ref. 8); –···–, Fujita *et al.* (Ref. 10); –····–, results obtained in the Glauber approximation at 500 eV (Ref. 10). Experimental data: +, Shibata *et al.* at 30 keV (Ref. 24); △, Konaka at 42 keV (Ref. 23); ⊙, Katase *et al.* at 1 keV (Ref. 1).

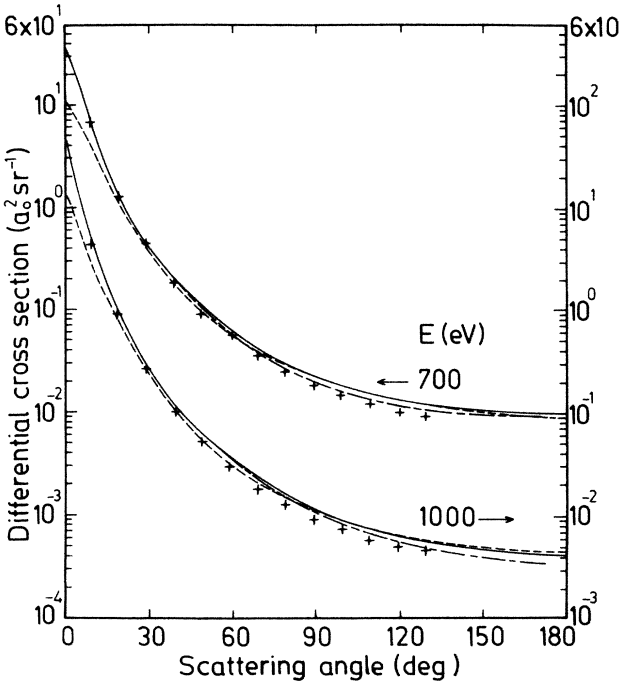

FIG. 6. Same legend as in Fig. 4 except at 700 and 1000 eV (note the arrows for scale).

Let us now examine the status of the results obtained in other models. The *SHP*2 and *SH* results are identical at all angles, indicating that the energy-dependent polarization potential [Eq. (2)] is not able to predict the forward peaking ($\theta \leq 30°$). However, in this angular region, the *SHP*1 and *SEP*1, which differ from the *SHP*2 only in treating the polarization potential in different way, i.e., including the correlation-polarization potential instead of the energy-dependent polarization potential [Eq. (2)], move in the right direction. At large scattering angles $\theta \geq 100°$ the *SHP*2 results merge with the *SHP*1 and *SEP*1. It is also seen that the Katase *et al.* and the *S* models fail in the forward direction due to the neglect of effects like polarization and exchange. It is interesting to compare the present *S* model and Katase *et al.* results which are on the same footing. The remarkable difference between two curves occurs at smaller ($\theta \leq 30°$) and higher ($\theta \geq 90°$) angles. The difference clearly reflects the quality of charge density (interaction potential) employed in the two calculations, as can be seen from the trend that the present *S* model predicts the shape and magnitude of DCS curve in better agreement to experimental data than those of Katase *et al.* model calculations.

At 200 eV the characteristics of the angular distribution changes from the dip structure at middle angles to almost a flat structure up to large angles. The present model calculations (*SHP*1 and *SEP*1) reproduce the experimental points very well up to $\theta \leq 60°$; thereafter they overestimate the experimental measurements. The situation regarding the results obtained in other models is the

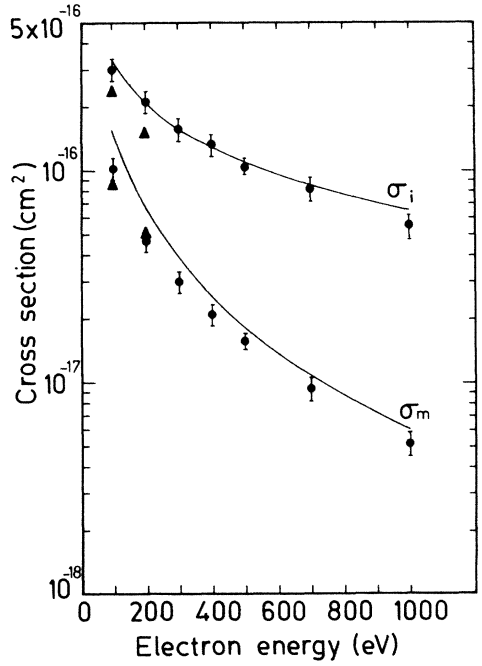

FIG. 8. Integral (σ_i) and momentum-transfer (σ_m) cross sections for e^--H_2O scattering as a function of electron energy. ——, *SHP*1 approximation (for notation see text). Experimental data: ⧫, Katase *et al.* (Ref. 1); ▲, Danjo and Nishimura (Ref. 2).

same as seen at 100 eV. The *SHP*2 and *S* results almost merge, each reflecting that the effect of the exchange potential is negligible at this energy. The model calculations of Katase *et al.* as usual underestimate the DCS's in the forward direction ($\theta \lesssim 30°$) and at large angles; their calculated values are higher by 70% than the measured values and are smaller by 30% than the present model calculations.

Figures 5 and 6 display the DCS's at higher energies of 300–500 eV and 700–1000 eV, respectively. The general trend of variation of the angular distribution is quite similar to that seen at 200 eV. As expected at such higher energies, the results of *SHP*1, *SEP*1, *SHP*2, and *S* almost become identical. The present results of Figs. 5 and 6 really correspond to a simple static approximation which agree very well with the measured values compared to the calculations of Katase *et al.*[1]

The DCS's have also been calculated as a function of the momentum transfer q in the Born and Glauber approximation by a number of authors[8–10] employing different degrees of sophistication in the bound-state molecular wave functions. Konaka[23] and Shibata *et al.*[24] have measured the total and elastic DCS for water molecules at 42 and 30 keV incident electrons energies, respectively. Figure 7 shows all the experimental results along with various theoretical calculations in Born and Glauber approximations. For the sake of comparison, we have also included in Fig. 7 the model calculations of Katase *et al.*[1] and the present *SHP*1 number at the highest energy, i.e., 1000 eV. The high-energy measurements due to Konaka[23] and Shibata *et al.*[24] were not absolute measurements and therefore, they were normalized to the value of $q \simeq 2.00$ a.u. by Katase *et al.* It is seen that all the calculations differ among themselves for $q < 2.00$ a.u. (i.e., in the small angular region). Beyond $q \geq 2.00$ a.u. all the curves including the present one are in agreement with the measurements. This clearly indicates that the calculated DCS's for energies up to 1000 eV are not expected to approach the high-energy limit, i.e., the Born approximation results. This finding is in agreement with the observation of Katase *et al.* In fact, the Born approximation would be valid for energies well above 1000 eV. However, for a quantitative assessment of the high-energy limit, the absolute DCS's need to be measured for the scattering of high-energy electrons.

B. Integral (σ_i) and momentum-transfer (σ_m) cross sections

In the present energy region the contribution from the nonspherical terms is not significant. Since we do not consider the dipole (which is responsible for infinite cross section at the zero angle in the present adiabatic-nuclei approximation) and higher-order terms in the optical potential, the integral cross sections are still finite and can be compared with experimental values where small-angle DCS's are not measured either. The forward-angle problem is not encountered in the corresponding momentum-transfer cross sections due to the $(1-\cos\theta)$ term. Figure 8 shows our σ_i and σ_m cross sections along with the calculated and experimentally observed values of Katase

TABLE I. Integral (σ_i) cross sections in various models for the e-H_2O scattering in units of 10^{-16} cm^2 (for notation see the text). Values in parentheses correspond to the percentage error in the experimental cross sections.

Energy (eV)	Present calculations				Experiment[a]
	S	*SHP*1	*SHP*2	*SEP*1	
100	2.29	3.37	2.68	3.40	2.98(12)
200	1.54	2.11	1.71	2.11	2.11(12)
300	1.22	1.59	1.32	1.59	1.56(12)
400	1.03	1.30	1.10	1.30	1.32(12)
500	0.882	1.11	0.930	1.11	1.04(9)
700	0.717	0.861	0.748	0.866	0.819(13)
1000	0.545	0.652	0.564	0.653	0.548(13)

[a] Reference 1.

TABLE II. Momentum-transfer (σ_m) cross sections in various models for e-H_2O scattering in units of 10^{-16} cm^2 (for notation see the text). Values in parentheses correspond to the percentage error in the cross sections.

Energy (eV)	Present calculations				Experiment[a]
	S	$SHP1$	$SHP2$	$SEP1$	
100	1.42	1.56	1.54	1.52	1.01(12)
200	0.621	0.668	0.665	0.651	0.464(12)
300	0.361	0.382	0.382	0.374	0.296(12)
400	0.240	0.252	0.253	0.247	0.208(12)
500	0.172	0.181	0.181	0.178	0.156(9)
700	0.104	0.108	0.109	0.106	0.0930(13)
1000	0.0589	0.0614	0.0613	0.0601	0.0515(13)

[a] Reference 1.

et al. and Danjo and Nishimura at 100–1000 eV. The measured values of σ_i and σ_m due to Katase *et al.*[1] are larger than those of Danjo and Nishimura[2] as is expected because of the differences in the magnitude of their angular distribution. We have also calculated the σ_i and σ_m in various models and the same are tabulated in Tables I and II, respectively. From these tables we see that the calculated values of σ_i and σ_m are not very sensitive to the choice of model potential approximation. Consequently, we have only shown on the curve the results obtained in one of our successful models, i.e., *SHP*1. It is clear from Table I that the present σ_i results are in very good agreement with experimental data of Ref. 1 at all energies considered here. For σ_m, the overall agreement between the calculated and the measured values is good except in the energy region of 100–400 eV, where the discrepency between the present theory and the experimental data is about 25%. We, however, expect some discrepancy between theory and experiment for these integral (σ_i,σ_m) cross sections due to the fact that the experimental points have to be extrapolated at small and large angles.

CONCLUSIONS

We finally conclude that a parameter-free model potential constructed for the full interaction of the collision system within the framework of the spherical-optical-potential approach is quite adequate to yield the elastic differential, integral, and momentum-transfer cross sections in the energy range of 100–1000 eV. It is also noted that in this energy range no other theoretical calculations exist for e-H_2O scattering which accounts for various physical effects (such as the polarization and exchange forces) playing important role. The calculated DCS's reproduced fairly well all the features of the experimental data. The integral and momentum-transfer cross sections were also reported and compared with recent measurements.

ACKNOWLEDGMENT

One of the authors (A.K.J.) gratefully acknowledges financial support from the Council of Scientific and Industrial Research (CSIR), New Delhi, India.

[1] A. Katase, K. Ishibashi, Y. Matsumoto, T. Sakae, S. Maezoho, E. Murakami, K. Watanabe, and H. Maki, J. Phys. B **19**, 2715 (1986).
[2] A. Danjo and H. Nishimura, J. Phys. Soc. Jpn. **54**, 1224 (1985).
[3] F. A. Gianturco and A. Jain, Phys. Rep. **143** (6), 347 (1986).
[4] S. Trajmar, D. F. Register, and A. Chutjain, Phys. Rep. **97(5)**, 219 (1983).
[5] K. Jung, Th. Antoni, R. Muller, K-H. Kochem, and H. Ehrhardt, J. Phys. B **15**, 3535 (1982).
[6] J. J. Olivero, R. W. Stagat, and A. E. Green, J. Geophys. Res. **77**, 4797 (1972).
[7] T. W. Shyn and S. A. Cho, Bull. Am. Phys. Soc. **32**, 1272 (1987).
[8] A. Szabo and N. S. Ostlund, J. Chem. Phys. **60**, 946 (1974).
[9] A. N. Tripathi and V. H. Smith, Jr., in *Comparison of Ab Initio Quantum Chemistry with Experiment: State-of-the-Art*, edited by R. Bartlett (Reidel, Dordrecht, 1985), p. 439, and references therein.
[10] T. Fujita, K. Ogura, and Y. Watanabe, J. Phys. Soc. Jpn. **52**, 811 (1983).
[11] A. Jain, Phys. Rev. A **34**, 3707 (1986); J. Phys. B **19**, L807 (1986).
[12] A. Jain, J. Chem. Phys. **86**, 1289 (1987).
[13] A. K. Jain, A. N. Tripathi, and A. Jain, J. Phys. B **20**, L389 (1987).
[14] D. G. Thompson and F. A. Gianturco, Chem. Phys. Lett. **14**, 110 (1976).
[15] F. A. Gianturco and S. Scialla, J. Phys. B **20**, 3171 (1987).
[16] N. T. Padial and D. W. Norcross, Phys. Rev. A **29**, 1590 (1984).
[17] F. A. Gianturco, A. Jain, and L. C. Pantano, J. Phys. B **20**, 571 (1987).
[18] B. L. Jhanwar and S. P. Khare, J. Phys. B **19**, L527 (1986).
[19] A. Jain, J. Chem. Phys. **78**, 6579 (1983); **81**, 724 (1984); S. N. Nahar and J. M. Wadehra, Phys. Rev. A **35**, 2051 (1987).
[20] F. W. Byron and C. J. Joachain, J. Phys. B **10**, 206 (1977).

[21]F. Calagero, *Variable Phase Approach to Potential Scattering* (Academic, New York, 1974).
[22]E. N. Lassettre and E. R. White, J. Chem. Phys. **60**, 2460 (1973).
[23]S. Konaka, J. Appl. Phys. Jpn. **11**, 1199 (1972).
[24]S. Shibata, N. Hirota, N. Kakuth, and T. Muramatsu, Int. J. Quantum Chem. **18**, 281 (1980).
[25]K. E. Banyard and N. H. March, J. Chem. Phys. **26**, 1416 (1957).
[26]B. S. Sharma and A. N. Tripathi, J. Phys. B **16**, 1827 (1983).